Journal of Inflammation Research

Dovepress
Taylor & Francis Group

Open Access Full Text Article

ORIGINAL RESEARCH

Exploring the Mechanism of CaoHuangGuiXiang Formula in Ameliorating Systemic *Candida albicans* Infection: A Study Integrating Network Pharmacology and Animal Experiments

Huizhen Yue[1,2,*], Shuhua Liu[1,*], Yinglu Bai[1], Wenjing Zhu[3], Jinhao Tian[3], Xiaolong Xu[1,2], Qingquan Liu[1,2]

[1]Department of Emergency and Critical Care, Beijing Hospital of Traditional Chinese Medicine, Capital Medical University, Beijing, People's Republic of China; [2]Research Laboratory of Infection and Immunity, Beijing Institute of Chinese Medicine, Beijing, People's Republic of China; [3]Clinical Medical College, Beijing University of Chinese Medicine, Beijing, People's Republic of China

*These authors contributed equally to this work

Correspondence: Xiaolong Xu; Qingquan Liu, Department of Emergency and Critical Care, Beijing Hospital of Traditional Chinese Medicine, Capital Medical University, Beijing, People's Republic of China, Email xiaolong_xu3013@126.com; liuqingquan_2003@126.com

Purpose: CaoHuangGuiXiang (CHGX) formula is a traditional Chinese medicine (TCM) used for the treatment of *Candida*-related infections. In this study, we adopted a comprehensive approach integrating network pharmacology and animal validation to investigate the potential targets and underlying mechanisms of the CHGX formula against systemic candidiasis.

Methods: Active ingredients and potential targets of CHGX were identified via the TCMSP, Swiss Target Prediction, and TCMID databases. Systemic *Candida* infection targets were retrieved from the GeneCards and OMIM databases. The protein-protein interaction (PPI) network of common targets was constructed via STRING, followed by topological analysis to identify hub nodes. Functional enrichment analyses were conducted via Metascape. Molecular docking studies were performed via AutoDock. A murine model of systemic *Candida albicans* infection was established to evaluate the therapeutic efficacy of CHGX formula.

Results: A total of 103 active compounds and 279 potential targets of the CHGX formula were identified, yielding 53 common targets between *Candida* infection-related targets and drug-related targets. Topological analysis of the PPI network identified 15 core targets, 25 significantly enriched KEGG pathways, and 38 enriched GO terms. Molecular docking studies demonstrated robust binding affinity between key CHGX compounds and the identified core targets. In vivo animal experiments revealed that CHGX significantly reduced mortality, improved body weight, mitigated renal pathology, decreased the kidney index, reduced the fungal burden, and alleviated tissue damage in systemic *Candida* infection. Furthermore, CHGX exerts immunomodulatory and anti-inflammatory effects by modulating macrophage and Th17/Treg cell populations, as well as by regulating cytokines levels.

Conclusion: This study elucidates the potential multi-pathway and multi-target mechanisms underlying the therapeutic efficacy of the CHGX formula against *Candida* infectious diseases, indicating its potential as a novel alternative antifungal drug and providing a scientific basis for its clinical application and further development.

Keywords: CaoHuangGuiXiang formula, systemic candidiasis, network pharmacology, antifungal activity, anti-inflammatory effect

Introduction

In recent years, the incidence of hospital-acquired fungal infections has risen sharply, with fungal infections becoming the leading cause of mortality from serious diseases such as AIDS and cancer. In the clinic, *Candida* species are the most common and important opportunistic microbes involved in fungal infection. Epidemiological data reveal that 50–70% of women experience vulvovaginal candidiasis at least once during their lifetime, with 5–8% developing recurrent infections that seriously affect their quality of life.[1] In addition, invasive candidiasis poses a major threat to sepsis, causing

Received: 2 July 2025
Accepted: 14 November 2025
Published: 9 December 2025

over 250,000 illnesses and more than 50,000 deaths globally.[2] CDC surveillance data indicate that candidemia is associated with an approximately 25% mortality rate among affected patients.[3] Furthermore, *Candida* infections necessitate prolonged treatment durations and extended hospitalizations, imposing substantial economic burdens on patients and healthcare facilities.[4] These high mortality rates and escalating healthcare costs not only threaten public health but also strain national medical budgets.

Currently, the therapeutic treatment for invasive fungal infections is limited to three primary classes of antifungal drugs: polyenes, azoles, and echinocandins. Despite their potential antifungal efficiency, these conventional agents are hindered by significant toxicity and recurrent drug resistance, particularly in critically ill patients, posing substantial challenges to clinical management.[5,6] Moreover, the extensive use of broad-spectrum agents in vulnerable populations undoubtedly accelerates the emergence of drug resistance, thereby exacerbating treatment failure rates and increasing mortality in candidaemia-related diseases.[7]

Given its diversity, availability, and reduced susceptibility to drug resistance, traditional Chinese medicine (TCM) offers a promising avenue for the development of novel antifungal agents. The CaoHuangGuiXiang (CHGX) formula, developed by Professor Qingquan Liu, a distinguished researcher in TCM prevention and treatment of infectious diseases, is an effective therapeutic prescription for managing *Candida*-related infections in critically ill patients.[8] Our prior investigations demonstrated that the CHGX formula exhibits potent antifungal activity against various *Candida* species, including the multidrug resistant *Candida auris*.[9,10] These studies revealed that the conserved Ras1-cAMP signaling pathway is pivotal in mediating CHGX-induced cell death in *Candida albicans*.[9] However, the comprehensive in vivo pharmacological mechanisms and the immunomodulatory role of the CHGX formula in combating *Candida* infection remain to be fully elucidated.

In this study, we employed an integrated approach combining network pharmacology and animal experimental validation to systemically elucidate the bioactive components, molecular targets, cellular signaling pathways, and immunomodulatory mechanisms of the CHGX formula against systemic candidiasis, providing scientific foundation for the clinical application and further development of the CHGX formula.

Materials and Methods

Network Pharmacological Analysis

Screening of the Main Active Components of the CHGX Formula

The chemical components of each herb in CHGX formula were retrieved from the Traditional Chinese Medicine Systems Pharmacology Database (TCMSP, http://lsp.nwu.edu.cn/tcmsp.php). The screening criteria included oral bioavailability (OB) ≥30%, drug-likeness (DL) ≥0.18, half-life ≥4, and Caco-2 cell permeability ≥-0.4 to identify major active compounds. Additional compounds were supplemented through literature reviews.

Collection of Drug Targets

The targets of the compounds were retrieved from the TCMSP database and DrugBank database (https://go.drugbank.com/). The UniProt database (https://www.uniprot.org/) was used to standardize target gene names to official symbols, yielding the potential therapeutic targets. The results from both databases were merged and deduplicated.

Construction of the Active Component-Target Network

Data on the active components and potential targets of CHGX were organized into two files: a network file (node relationships) and a node classification file. These files were imported into Cytoscape 3.7.0 (https://cytoscape.org/) to construct an "active component-target" network. Topological analysis was performed to evaluate network properties.

Acquisition of Candidiasis-Related Targets

Potential targets associated with systemic candidiasis were obtained by searching the OMIM (https://omim.org/) and GeneCards Suite (https://www.genecards.org/) databases with "Candidiasis" as the keyword. The results from both databases were merged and deduplicated.

Identification of Overlapping Targets Between Drugs and Diseases

The overlapping targets between the CHGX formula and systemic *Candida* infection were identified via the Venny online platform (https://www.bioinformatics.com.cn/). These intersection targets represent potential therapeutic targets for treating candidiasis.

Protein-Protein Interaction (PPI) Network Construction

The overlapping targets were imported into the STRING database (https://string-db.org/) with the species specified as *Homo sapiens* and a confidence score of 0.7 (high confidence). The resulting PPI network file ("string_interaction.tsv") was imported into Cytoscape 3.7.0 for topological analysis. Core targets were identified on the basis of degree and betweenness centrality.

GO and KEGG Pathway Enrichment Analysis

The Metascape database (https://Metascape.org/) was used to perform Gene Ontology (GO) and Kyoto Encyclopedia of Genes and Genomes (KEGG) enrichment analyses. The overlapped target genes were entered into the Metascape database, and the species was specified as *Homo sapiens*. GO analysis covered biological processes (BPs), cellular components (CCs), and molecular functions (MFs). KEGG analysis identified signaling pathways potentially involved in treating candidiasis. The top 10 BPs, CCs and MFs and the top 20 pathways were functionally enriched and visualized via the enrichment dot bubble online platform (https://www.bioinformatics.com.cn/).

Construction of the Drug-Disease-Target-Pathway Network

Based on the results of KEGG enrichment analysis, the top 20 pathways were selected to construct a network integrating the CHGX formula, candidiasis targets, and pathways. Data on the active components, core targets and pathways were organized into two files: a network file (node relationships) and a node classification file. These files were imported into Cytoscape 3.7.0 to construct an "drug-disease-target-pathway" network. Network topology parameters (degree, betweenness, and closeness) were analyzed to identify key active components and core targets.

Molecular Docking Validation

Key target proteins identified from PPI network and "drug-disease-target-pathway" network were selected for molecular docking with corresponding active compounds. 7 core targets with high degree values were selected. Their 3D protein structures were downloaded from the PDB database (http://www.rcsb.org/) in PDB format. 10 key active compounds of the CHGX formula were retrieved from PubChem (https://pubchem.ncbi.nlm.nih.gov/) and converted to MOL2 format. Using AutoDock Vina (http://vina.scripps.edu/), molecular docking was performed after protein preprocessing (removing water molecules, adding hydrogen atoms, optimizing energy, and adjusting force field parameters). The docking results were visualized and analyzed with PyMOL software.

Animal Experimental Validation

Strains and Cultivation

The fungal strain used in this study was *C. albicans* SC5314. A yeast extract peptone dextrose(YPD) medium (2% glucose, 2% peptone, and 1% yeast extract) was used for the routine growth of fungal cells. YPD medium containing 100 mg/L ampicillin and 100 mg/L kanamycin was used for the fungal burden assay.

Preparation of CHGX Water-Decoction

The CHGX formula (50 g) consists of the roots and rhizomes of *Glycyrrhiza uralensis Fisch*. ex DC. [Fabaceae] (Gan Cao, 15 g), the roots and rhizomes of *Rheum palmatum L*. [Polygonaceae] (Da Huang 10 g, 2103137), the bark of *Neolitsea cassia (L). Kosterm*. [Lauraceae] (Rou Gui, 10 g), and the aerial part of *Pogostemon cablin (Blanco) Benth* (Guang Huo Xiang, 15 g). Among, *Glycyrrhiza uralensis* Fisch. ex DC. [Fabaceae] was originated from Gansu Province, China (Voucher number 211209002, Beijing KangYuanXiangRui Pharmaceutical Technology Co., LTD). *Rheum palmatum* L. [Polygonaceae] was originated from Qinghai Province, China (Voucher number 2103137, Beijing ShengShiLong pharmaceutical Co., LTD). *Neolitsea cassia* (L). Kosterm. [Lauraceae] was originated from Guangxi Province, China (Voucher number 21081303, Beijing Xinglin pharmaceutical Co., LTD). *Pogostemon cablin* (Blanco) Benth was

originated from Guangdong Province, China (Voucher number 2108079, Beijing ShengShiLong pharmaceutical Co., LTD). These herbs were provided by the pharmacy of the Beijing Hospital of Traditional Chinese Medicine (Beijing, China), which accorded with general technical requirements of Chinese Pharmacopoeia and followed the standard of Beijing Specifications for the Processing of Traditional Chinese Medicinal Preparations (2023 Edition).

The CHGX water decoction was prepared through a standardized extraction process as previously reported.[9,10] Initially, 100 g of raw CHGX herbal material was soaked in 600 mL of deionized water for 30 minutes, followed by a 30-minute decoction process to obtain the primary aqueous extract. The residual material was subsequently redecocted with 400 mL of deionized water for 20 minutes to yield the secondary extract. Both decoctions were combined and concentrated under reduced pressure to a final volume of 100 mL (1 g crude herbs/mL, 100% w/v), referred to as the CHGX water-decoction.

Animals and Ethics Statement

BALB/c mice (female, 18–20 g, 6 weeks old) were purchased from SiBeiFu Bioscience Co., Ltd. (Beijing, China). All experiments were conducted in accordance with the National Institutes of Health Guide for the Care and Use of Laboratory Animals (NIH Publications No.8023, revised 1978). In addition, all protocols in this study were approved with the permission of the Beijing Institute of Chinese Medicine, Ethics Committee (permit No. 2023–02-57).

Systemic Mouse Infection Model

Systemic candidiasis infection caused by *C. albicans* (SC5314) was established in a murine model according to previous reports.[9] The mice were randomly divided into 4 groups: sham group, model group, CHGX group, and fluconazole (FLU) group, with 10 mice in each group. Fungal cells of SC5314 were initially cultured on solid YPD medium plates at 37 °C for 2 days. Fungal cells from a single colony were inoculated into liquid YPD medium at 30 °C with shaking overnight. Fungal cells were harvested, washed, and suspended in PBS.

For survival rate analysis, the mice in the model group, CHGX group, and FLU group were immunosuppressed by intraperitoneal injection of cyclophosphamide (100 mg/kg) 1 day before infection and then intravenously injected with 1×10^6 or 5×10^5 SC5314 cells in 200 ul of PBS via the tail vein. After infection, mice in the CHGX group were orally administered 6.5 g/kg/day CHGX water-decoction for 7 days, and the mice in the FLU group were orally administered 25 mg/kg/day fluconazole. The mice in the control and model groups were treated with solvent. The mortality of the mice in each group was monitored and recorded daily.

For the fungal burden and histopathological assays, fungal cells of SC5314 were adjusted to 1×10^8 cells/mL in PBS. The mice in the model group, CHGX group, and FLU group were infected with 2×10^7 SC5314 cells in 200 ul of PBS by intraperitoneal injection. After infection, the mice in the CHGX group were orally administered with 6.5 g/kg/day CHGX water-decoction for 7 days, and mice in the FLU group were orally administered 25 mg/kg/day fluconazole. The mice in the control and model groups were treated with solvent. For the fungal burden assay, the mice were euthanized via cervical dislocation on day 7 post-infection. The kidneys were harvested, weighed and homogenized. The kidney suspensions were diluted and plated onto YPD medium supplemented with 100 mg/L ampicillin and 100 mg/L kanamycin for the colony-forming unit (CFU) analysis. For evaluation of the kidney index, kidneys were harvested and weighed. The kidney index was calculated as [kidney weight (g)/body weight (g)] ×100%, which indicates inflammation and edema in the kidney. For the histopathological assay, kidneys were harvested and fixed with 10% (weight/volume) buffered formalin, washed, dehydrated, and embedded in paraffin wax, as previously described. The samples were sectioned and stained with Hematoxylin-eosin (H&E) and periodic acid–Schiff (PAS) for microscopy.

Flow Cytometry Assay

Flow cytometry assays of macrophages and Th cells were performed according to a previous report.[11] First, the peripheral blood of the mice was collected in EDTA/heparin tubes and pre-chilled RBC lysis buffer (Tonbo; TNB-4300-L100) was added and incubated for 10 min at room temperature in the dark. Then, the samples were centrifuged at 350 × *g* for 5 minutes, and the mononuclear immune cells were collected. For cell surface staining, the collected cells were washed twice with PBS followed by incubation with live/dead staining (Tonbo; 13–0865-

T100) diluted at 1:100 with PBS. Then, the cells were washed with flow staining buffer, blocked with Fc receptors and incubated with antibodies. The concentration and dilution ratio of the antibodies was in accordance with the instructions for use. Among, FITC anti-CD45 (Tonbo; 35–0451-U025, 1:100), PE anti-CD11b (Tonbo; 50–0112-U100, 1:160) and APC anti-F4/80 (Tonbo; 20–4801-U100, 1:40) antibodies were used for macrophages surface staining. Additionally, Percp-Cy5.5 anti-CD45 (Tonbo; 65–0451-U025, 1:160), FITC anti-CD4 (Tonbo; 35–0042-U025, 1:200), RedFlour 710 anti-CD3 (Tonbo; 80–0032-U025, 1:40), PE-CY7 anti-CD25 (Tonbo; 60–0251-U025, 160), PE anti-IL17A (Invitrogen; 12–7177-81, 1:160), and APC anti-Foxp3 (Tonbo; TNB-0607-KIT, 1:160) antibodies were used for Th cell surface staining. After staining, the cells were washed twice with PBS and resuspended. Samples were acquired using a Thermo Fisher Attune flow cytometer, and the data were analyzed via FlowJo software.

Mouse Cytokine Assay

The mouse cytokine assay was conducted as previously reported with slight modifications.[12] Serum was harvested from each group to detect the concentrations of 17 cytokines including interleukin- (IL-) 1β, IL-2, IL-4, IL-5, IL-6, IL-9, IL-10, IL-12p70, IL-13, IL-17A, IL-18, IL-22, IL-23, IL-27, interferon-gamma (IFN-γ), tumor necrosis factor-α (TNF-α), and granulocyte-macrophage colony-stimulating factor (GM-CSF) using a ProcartaPlex 17plex kit (Invitrogen; EPX170-26087-901). The assay was performed and analyzed by Laizee Biotech (Shanghai, China) via Luminex200 instrument and ProcartaPlex Analyst 1.0 software. In brief, 25 μL of each sample was incubated for 2 hours with 25 μL of 1X detection antibody mixture of color-coded beads pre-coated with analyte-specific capture antibodies. After washing, biotinylated detection antibodies specific to all analytes of interest were added to form an antibody-antigen sandwich, and then, phycoerythrin-conjugated streptavidin was added to bind the biotinylated detection antibodies. The beads were read on a Luminex 200 analyzer. One laser was used to classify the bead and determine each analyte. The second laser was used to determine the magnitude of the PE-derived signal, which was directly proportional to the amount of analyte bound. Standard curves for all 17 analytes were generated, and the concentration level of each analyte was determined via ProcartaPlex Analyst 1.0 software.

Statistical Analysis

The statistical software SigmaStat package (SPSS 26.0 Inc.). was used for data analysis. Values were presented as mean ± standard deviation (SD). One-way analysis of variance (ANOVA) was performed to compare statistical differences with multiple groups and student's *t*-test was performed between two groups. Survival curves were performed using log-rank analysis (Mantel-Cox). $p < 0.05$ was considered statistically significant.

Results

Exploration of the Active Components and Targets of the CHGX Formula

A total of 103 active components were identified from CHGX formula through the TCMSP database and literature reviews (Table S1). These components were derived from four key herbs in the formula: 71 components originated from *Glycyrrhiza uralensis Fisch*. ex DC. [Fabaceae], 12 from *Rheum palmatum L*. [Polygonaceae], 11 from *Neolitsea cassia (L). Kosterm*. [Lauraceae], and 10 from *Pogostemon cablin* (Blanco) Benth. Notably, quercetin was identified as a common active component between *Glycyrrhiza uralensis* and *Pogostemon cablin*. Furthermore, potential targets of these active components were retrieved from the TCMSP database and DrugBank database, and the corresponding gene entries were standardized and integrated with the UniProt database entries, yielding a total of 279 target genes.

To elucidate the relationships between the active components and their potential targets, we constructed a "Compound-Target" network using Cytoscape 3.7.0 software. Following the removal of isolated nodes, the network comprised 386 nodes and 1858 edges (Figure 1). Based on their degree values, we identified the top 12 active components, including quercetin, kaempferol, oleic acid, 7-methoxy-2-methylisoflavone, formononetin, β-sitosterol, naringenin, emodin, medicarpin, isorhamnetin, licochalcone, and chitin.

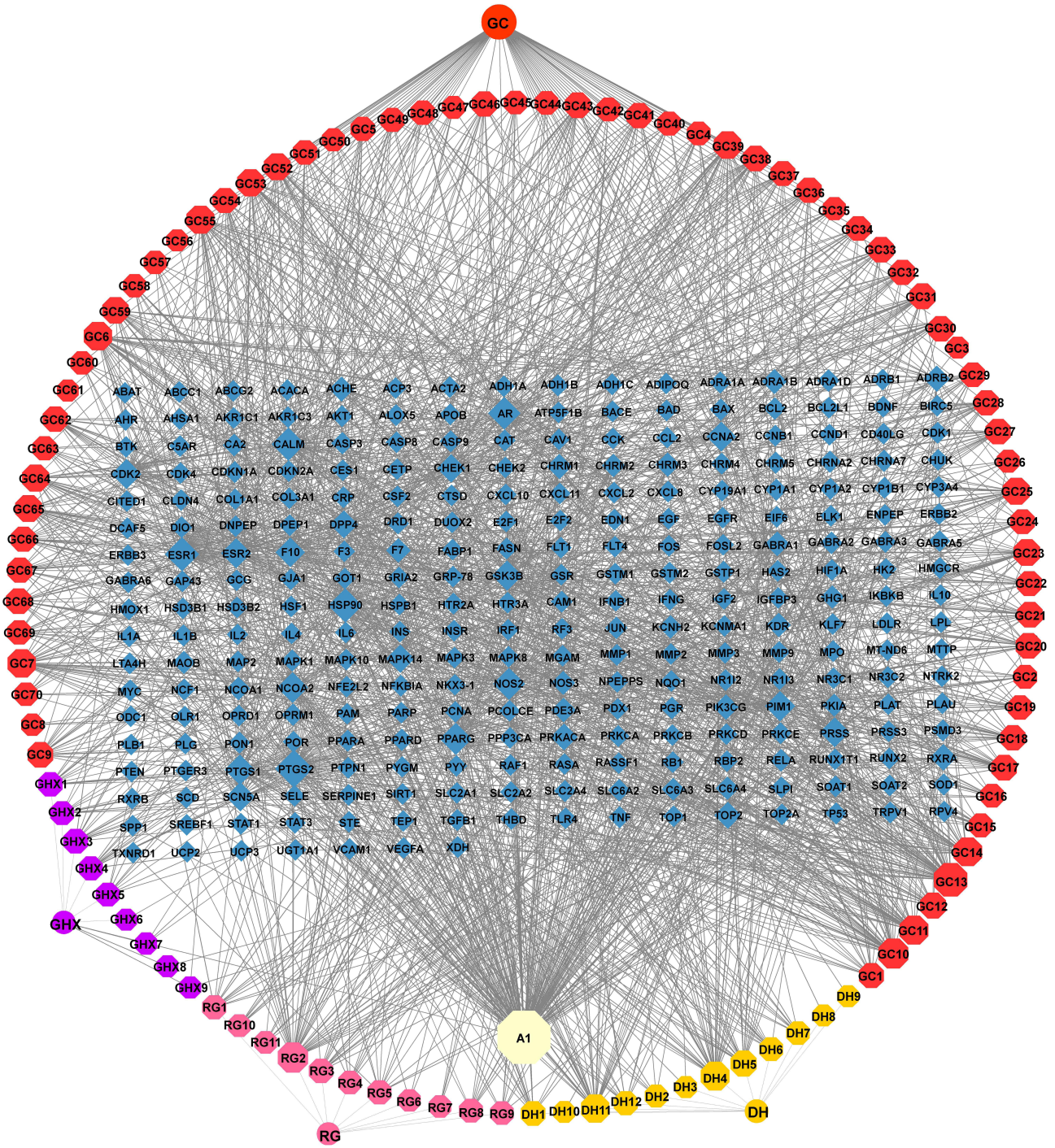

Figure 1 Network diagram of drug components and potential targets. The blue prisms represent potential targets and the hexagons represent active components of the CHGX formula. The lines illustrate the interactions between active components and potential targets. Additionally, hexagons colored red, purple, pink and yellow specifically indicate active ingredients derived from Gan Cao (GC), Guang Huo Xiang (GHX), Rou Gui (RG) and Da Huang (DH), respectively. The beige hexagon "A1" indicates an ingredient shared between GC and GHX.

Collection of Disease-Related Genes and Construction of the PPI Network

A total of 774 genes associated with systemic candidiasis were retrieved from GeneCards and OMIM databases, after removing the repeated entries. Through cross-comparison between the disease-related targets and active compound-related targets, 53 overlapping targets were identified (Figure 2A and Table S2), which are considered as the potential therapeutic candidates for systemic candidiasis.

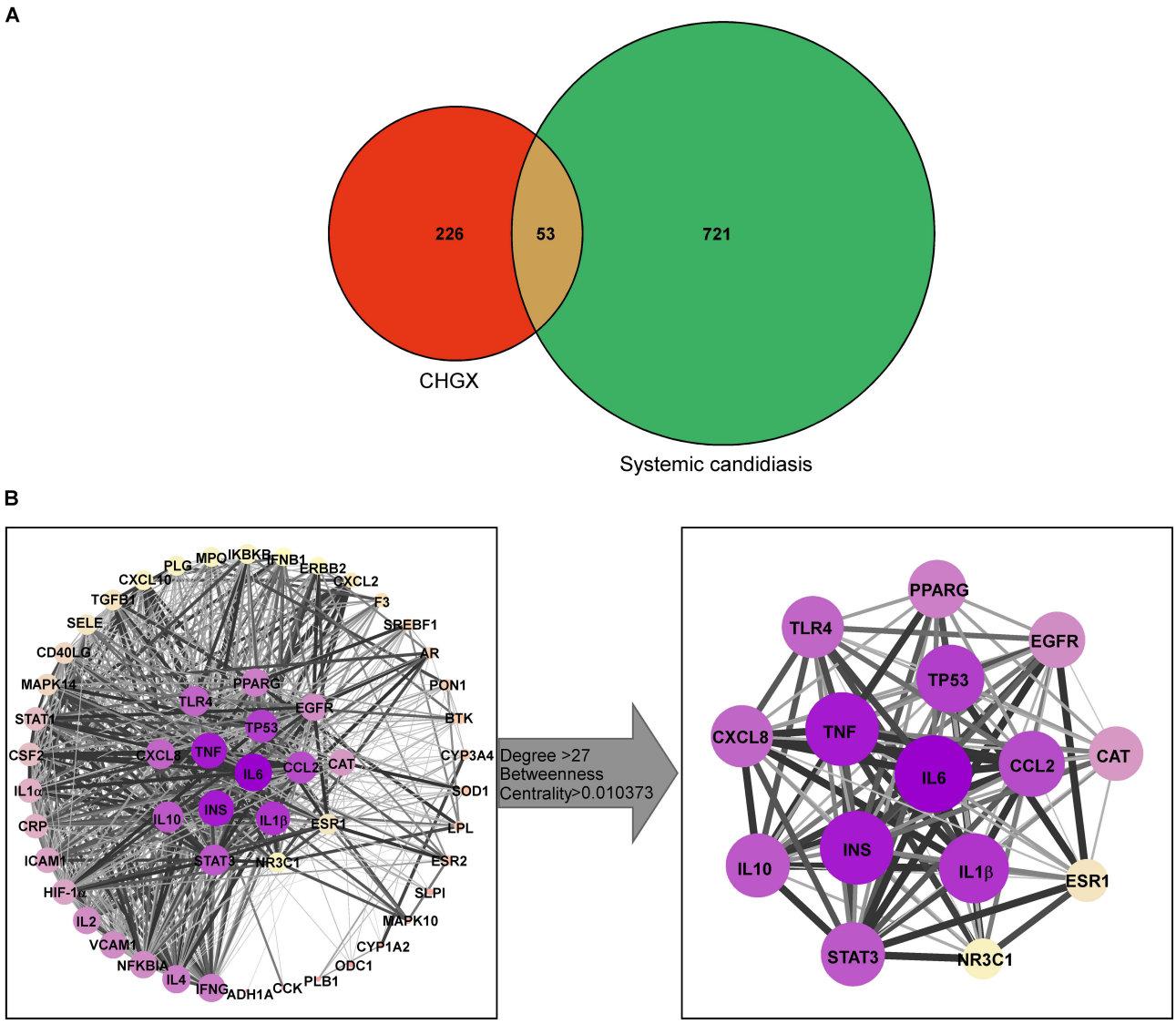

Figure 2 Potential therapeutic targets of the CHGX formula in treatment of systemic candidiasis. (**A**) Venn diagram depicting the overlap of potential targets between the CHGX formula and systemic candidiasis disease. (**B**) Protein-protein interaction (PPI) networks. The left network displays the interactions among 53 potential targets shared between the CHGX formula and systemic candidiasis. The right network highlights the top 15 key targets based on their degree and betweenness centrality values.

The 53 overlapping targets were imported into the STRING database to generate a PPI network comprising 53 nodes and 711 edges (Figure 2B). In this network, nodes represent target proteins, whereas edges depict their interactions, with edge thickness proportionally indicating the interaction strength. Based on topological parameters, including degree and betweenness centrality, the top 15 core targets were selected to construct the PPI sub-network, revealing that IL-6, IL-1β, INS, TNF, TP53, and CCL2 were among the most densely interconnected nodes within the network (Table S3).

GO and KEGG Enrichment Analysis

To elucidate the mechanisms underlying the therapeutic effects of the CHGX formula against systemic candidiasis, we performed GO functional enrichment analysis on 53 overlapping targets via the Metascape database. A total of 956 biological processes (BPs), 22 cellular components (CCs), 72 molecular functions (MFs), and 135 KEGG pathways were annotated, with the top 10 significantly enriched terms in the BP, CC and MF categories visualized in Figure 3A. The key BPs included cellular response to cytokine stimulus, inflammatory response, positive regulation of cytokine production, cytokine-mediated signaling pathway, and cell activation. The core CCs included the external side of the plasma membrane, vesicle lumen, side

https://doi.org/10.2147/JIR.S551135

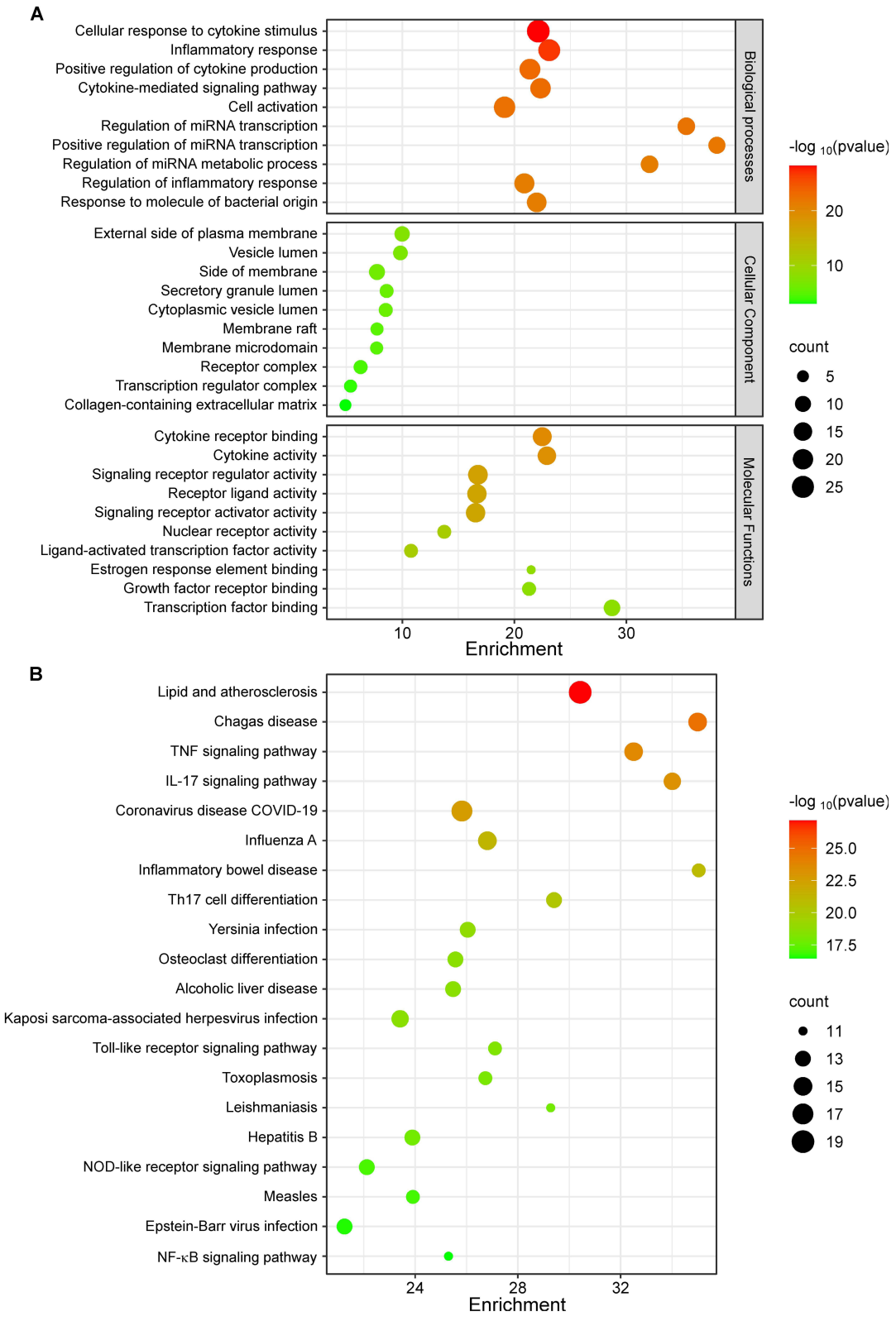

Figure 3 Functional analysis of common targets between CHGX and systemic candidiasis. (**A**) Gene Ontology (GO) enrichment analysis revealing the enriched biological processes, cellular components, and molecular functions associated with the common targets. (**B**) Kyoto Encyclopedia of Genes and Genomes (KEGG) pathway analysis highlighting significantly enriched pathways among the common targets.

of the membrane, secretory granule lumen, and cytoplasmic vesicle lumen. Notable MFs included those associated with cytokine receptor binding, cytokine activity, signaling receptor regulator activity, receptor-ligand activity, and signaling receptor activator activity. Additionally, the top 20 enriched pathways such as lipid and atherosclerosis, the TNF signaling pathway, the IL-17 signaling pathway, Th17 cell differentiation, and the Toll-like receptor signaling pathway are illustrated in Figure 3B. To further understand the intricate relationships among drugs, diseases, targets, and pathways, we constructed a multi-dimensional "drug-disease-target-pathway" network using Cytoscape software, where prisms represent active components, hexagons represent critical targets, and V-shapes represent signaling pathways (Figure 4).

Molecular Docking Analysis

Based on the insights derived from the PPI network and "drug-disease-target-pathway" network analyses, 7 core target proteins with 10 key active components were selected for molecular docking studies (Figure 5). The binding energy and root

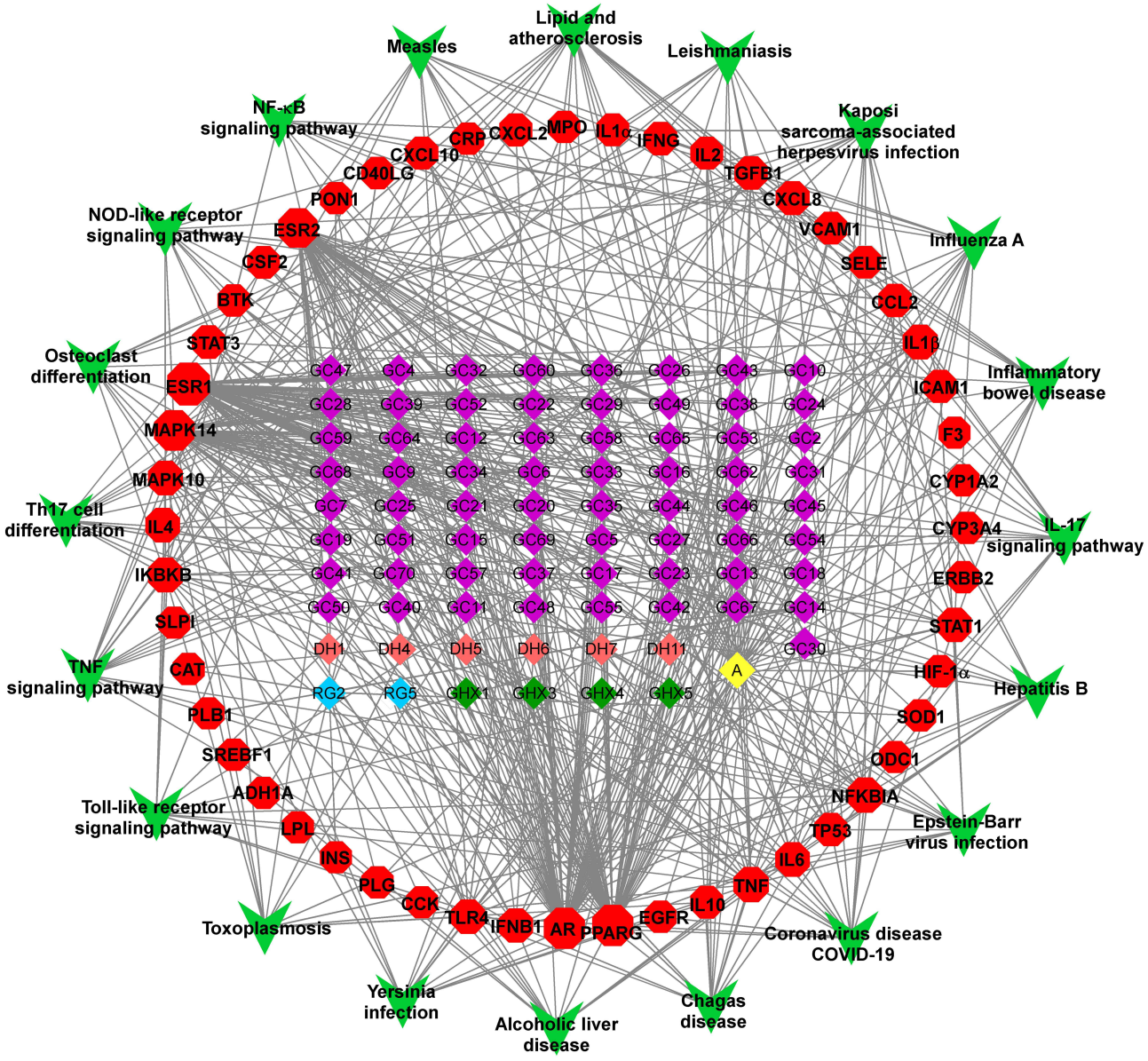

Figure 4 CHGX-target-disease-pathway network. The prisms represent active components of the CHGX formula. Specifically, purple, pink, blue and green prisms represent the active components derived from GC, DH, RG and GHX, respectively. The yellow prism represents a shared ingredient between GC and GHX. The red hexagons indicate potential targets and the green V-shapes indicate enriched signaling pathways associated with the CHGX formula and systemic candidiasis.

https://doi.org/10.2147/JIR.S551135

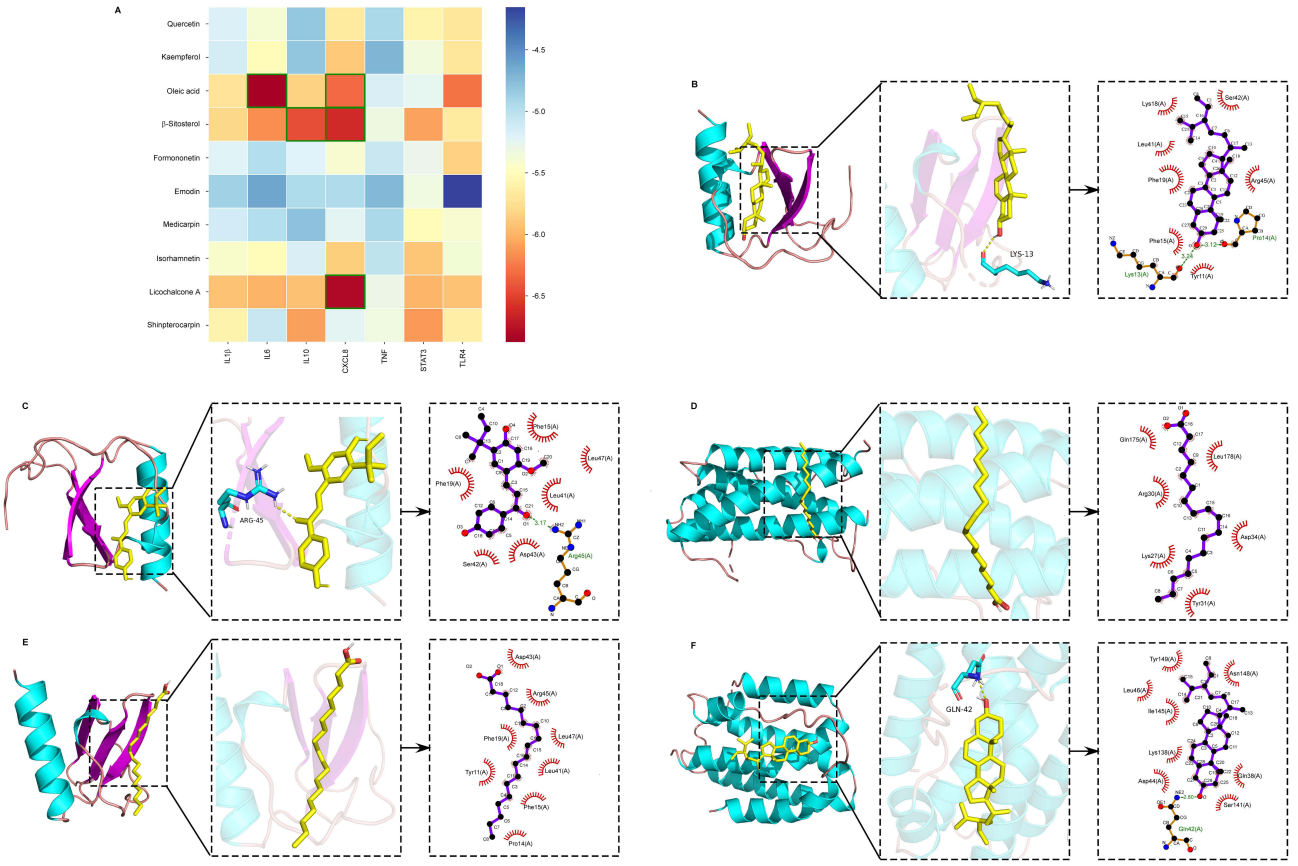

Figure 5 Molecular docking analysis. (**A**) Heat-map illustrating the docking binding energy of key components and core targets. The binding energy is color-coded, with lower values indicating stronger binding affinity. The green boxes represent the binding energy is lower than −6.3 kcal/mol. (**B**) Molecular docking pattern of β-sitosterol and CXCL8. (**C**) Molecular docking pattern of licochalcone A and CXCL8. (**D**) Molecular docking pattern of oleic acid and IL-6. (**E**) Molecular docking pattern of oleic acid and CXCL8. (**F**) Molecular docking pattern of β-sitosterol and IL-10. The yellow dotted line represents hydrogen bonds.

mean square deviation (RMSD) values which were calculated to evaluate the binding affinity and stability between the compounds and their respective target proteins, are provided in Tables S4 and S5. Generally, the lower the binding energy, the greater the binding stability, with a threshold of less than −5 kcal/mol indicating a significant docking interaction. As shown in Figure 5A, the molecular binding energy between β-sitosterol and CXCL8, licochalcone A and CXCL8, oleic acid and IL-6, oleic acid and CXCL8, β-sitosterol and IL-10 were less than −6.3 kcal/mol, indicating that these components can bind to the active sites of their targets. The corresponding molecular docking patterns were visualized using PyMOL software, demonstrating the stable conformation between small molecular and target proteins with intermolecular forces such as hydrogen bonding (Figure 5B–F).

CHGX Formula Enhances the Survival Rate of Systemic Candidiasis Model Mice

Systemic candidiasis is clinically characterized by severe morbidity and high mortality. In immunocompromised mice, systemic infection with *C. albicans* resulted in 100% mortality within 4 days, irrespective of the inoculation dose (1×10^6 or 5×10^5 CFUs) (Figure 6A and B). Our study demonstrated that the treatment of CHGX conferred a survival advantage to mice infected with a low dose of *C. albicans*. As showed in Figure 6B, survival analysis indicated that both CHGX and FLU treatment significantly improved the 7-day survival rate compared with that of the model mice, with rates reaching 40% and 100%, respectively.

CHGX Formula Reduces Renal Fungal Burden and Ameliorates Kidney Injury in Systemic Candidiasis Mice

As shown in Figure 7A, compared with the sham group, the mice exhibited substantial weight loss in the model group. Notably, treatment with CHGX and FLU significantly ameliorated this weight loss in infected mice. Consistent with the

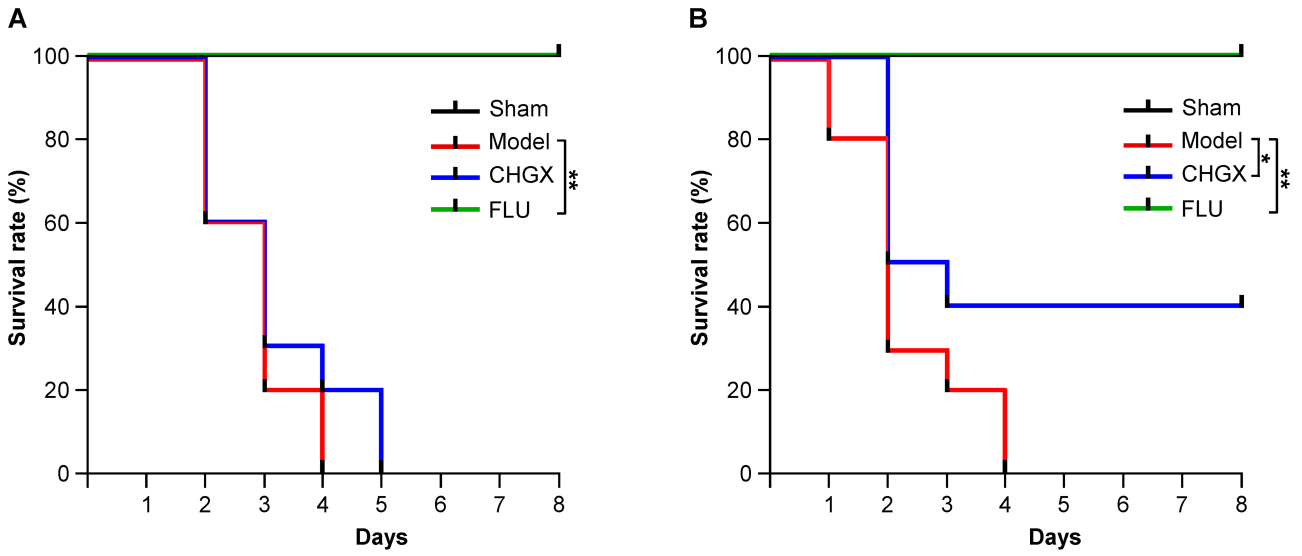

Figure 6 Kaplan–Meier survival curves for systemic candidiasis mice. (**A**) Survival analysis of mice in the CHGX and FLU groups following intravenous injection of 1×10^6 cells of *C. albicans* SC5314. (**B**) Survival analysis of mice in the CHGX and FLU groups following intravenous injection of 5×10^5 SC5314 cells. Each group has ten mice, and mortality was monitored and recorded daily. *p < 0.05 or **p < 0.01 was considered statistically significant.

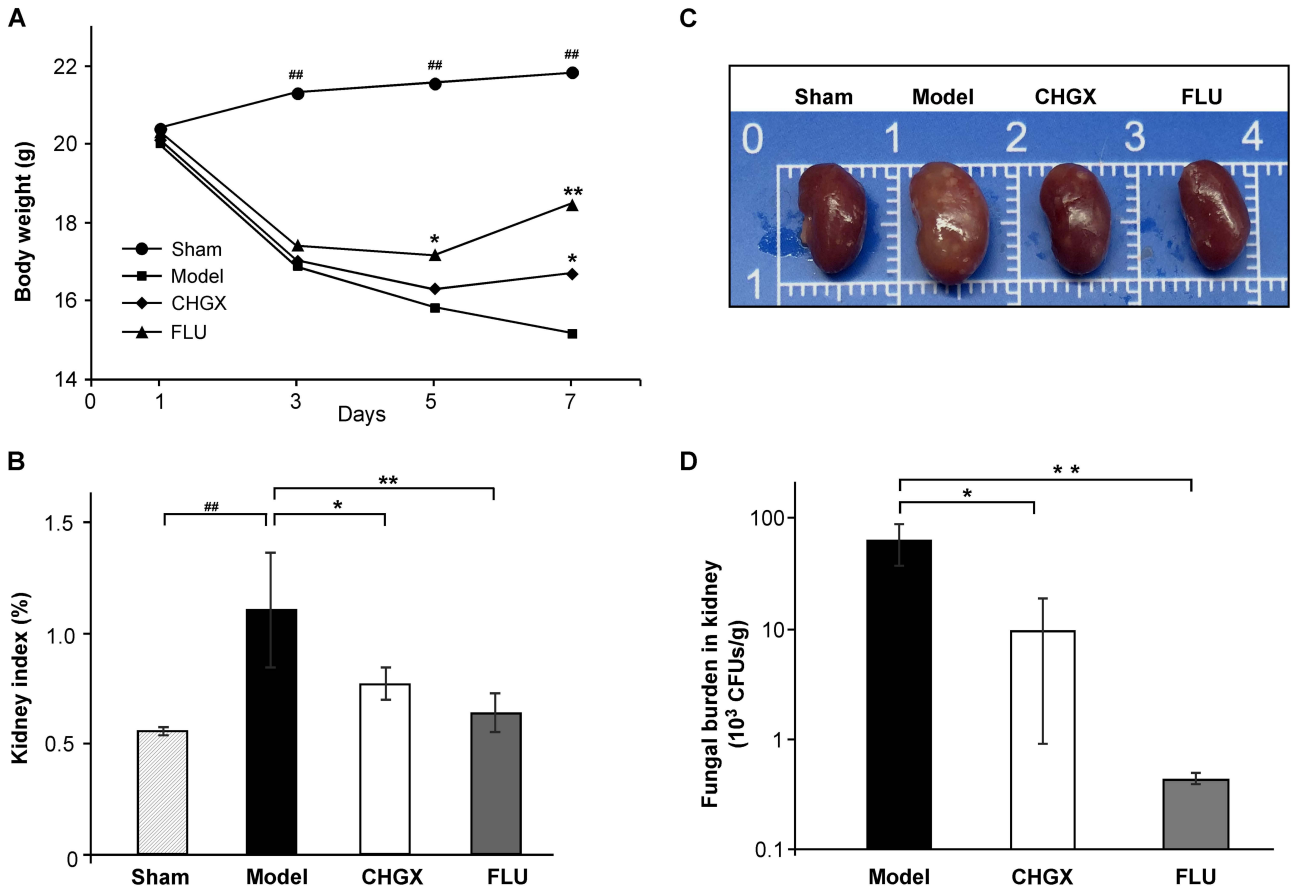

Figure 7 Pharmacodynamic results. (**A**) The body weights of the mice were monitored daily (n=6). (**B**) The kidney index was calculated as [kidney weight (g) / body weight (g)] × 100% (n=4). (**C**) Representative images of mouse kidneys. (**D**) Fungal burden in the kidney. Kidneys were harvested, weighed and homogenized for CUFs analysis on day 7 post-infection (n=4). The data are presented as (mean ± SD). ##p < 0.01 indicates significant difference in contrast to the sham group. *p < 0.05 or **p < 0.01 indicate significant differences in contrast to the model group.

https://doi.org/10.2147/JIR.S551135

observed changes in body weight, the kidney index was markedly lower following treatment with both CHGX and FLU (Figure 7B and C), indicating that the CHGX formula effectively protected mice from *C. albicans*-induced damage. Furthermore, we evaluated the impact of the CHGX formula on the renal fungal burden. As illustrated in Figure 7D, FLU treatment significantly suppressed fungal proliferation in the kidney tissues of infected mice compared with the model group. Moreover, a notably lower fungal burden was observed in the mice treated with CHGX, suggesting that the CHGX formula has an effective antifungal activity within the host body.

To assess kidney injury directly, PAS and H&E staining were performed. As shown in Figure 8, the mice in the model group exhibited pronounced kidney lesions, including edema, glomerular injury, and inflammatory cell infiltration. Following treatment with the CHGX formula, the pathological changes in the kidney tissues were significantly alleviated, with a marked reduction in edema and inflammatory cells, along with the restoration of glomerular structure. Consistent with the findings regarding the renal fungal burden, the level of fungal colonization in mice treated with the CHGX formula was significantly lower than that in the model group. Collectively, these results indicate that the CHGX formula exhibits a protective effect against tissue damage in systemic candidiasis mice.

The CHGX Formula Exerts an Anti-Inflammatory Effect on Systemic Candidiasis Mice

Macrophages and T helper (Th) cells play critical roles as effector cells in host defense against *Candida* infections.[13–15] In this study, we aimed to elucidate the immunoregulatory function of macrophages and Th cells in systemic candidiasis following treatment with the CHGX formula. As shown in Figure 9A and B, the proportion of macrophages was significantly elevated in the CHGX group compared to the model group. In contrast, the level of Th17 cells was slightly lower in the CHGX group than in the model group (Figure 9C and D). Notably, the proportion of regulatory T (Treg) cells was significantly increased in the CHGX group than in the model group (Figure 9E and F). These results suggest that the CHGX formula may be involved in the regulation of macrophages and Treg cells in the defense against systemic candidiasis.

Furthermore, we observed that the levels of pro-inflammatory cytokines, including IL-2, IL-5, IL-6, IL-17A, IL-18, TNF-α, and IFN-γ, were significantly upregulated in the model group than in the sham group (Figure 10A–G). However, the levels of these pro-inflammatory cytokines were markedly reduced in the CHGX group, indicating that CHGX plays a crucial role in inhibiting inflammatory factors. Additionally, the level of IL-4, an anti-inflammatory cytokine, was

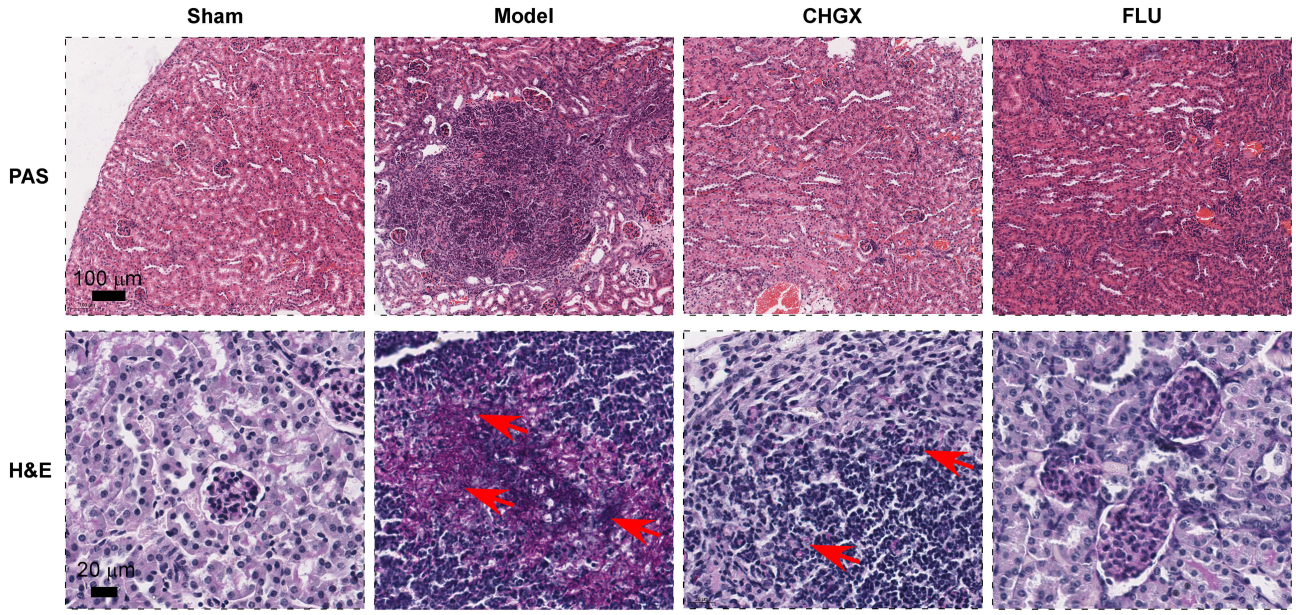

Figure 8 Histological analysis of mouse kidneys via Periodic acid–schiff (PAS) and Hematoxylin-eosin (H&E) staining. The red arrows highlight fungal colonization by *C. albicans* in the kidney.

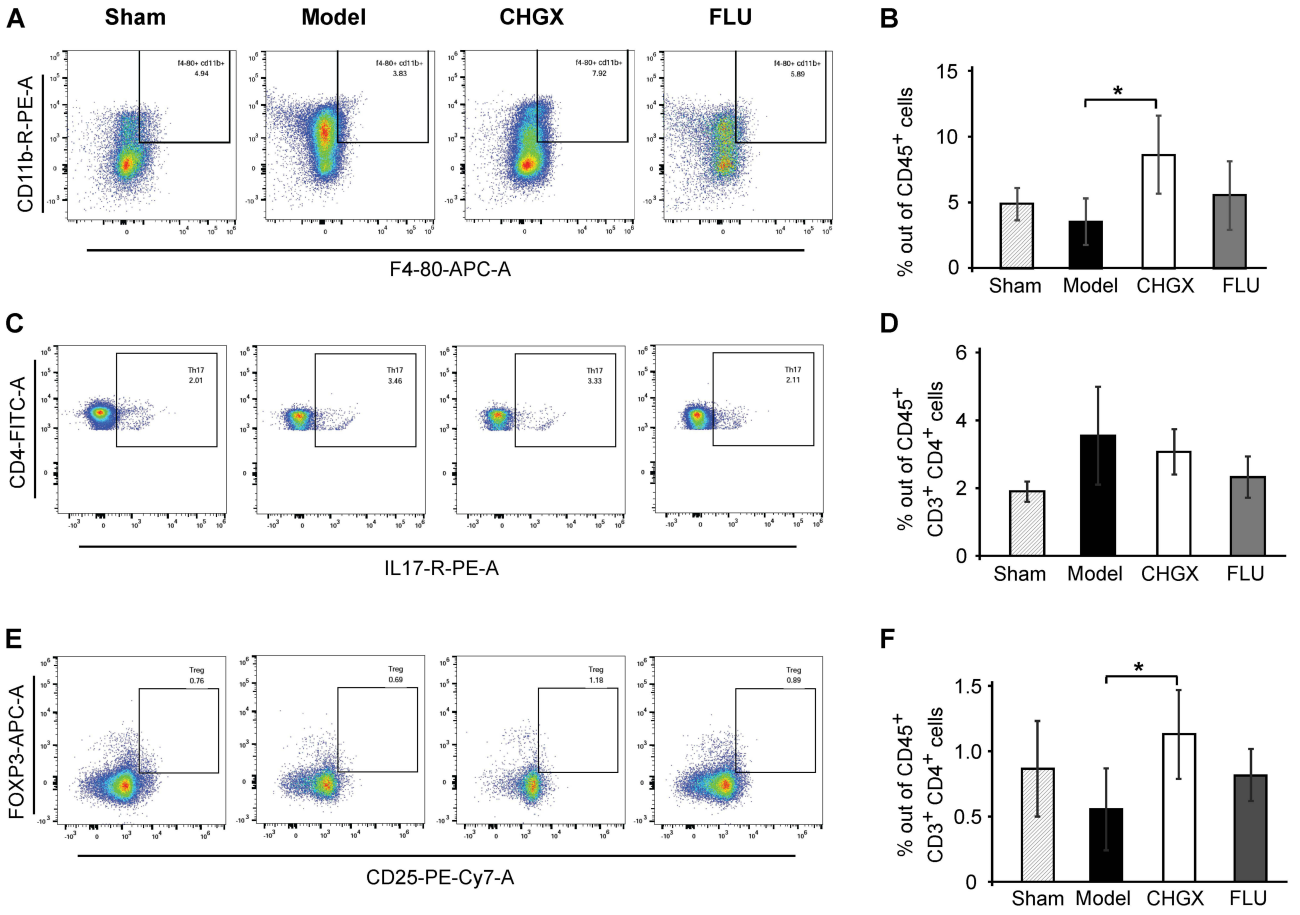

Figure 9 Flow cytometry assay. (**A** and **B**) Quantification of macrophages. (**C** and **D**) Quantification of Th17 cells. (**E** and **F**) Quantification of Treg cells. The data are presented as (mean ± SD). *$p < 0.05$ indicate significant differences compared with the model group.

significantly decreased in the model group but notably increased in the CHGX group (Figure 10H), suggesting that the CHGX formula exerts an anti-inflammatory effect by modulating the expression of inflammatory cytokines.

Discussion

Systemic candidiasis, a potentially fatal fungal infection, is particularly prevalent among immunocompromised individuals. Due to its propensity for disseminated organ damage and dysregulated immune responses, it commonly leads to high morbidity and mortality.[16,17] Despite advancements in antifungal therapies, significant challenges still persist, including the emergence of drug resistance and immune dysfunction, underscoring the urgent need for innovative therapeutic approaches. The CHGX formula, a traditional Chinese medicine, is composed of *Glycyrrhiza uralensis, Rheum palmatum, Neolitsea cassia*, and *Pogostemon cablin*. Our integrated systems pharmacology analysis coupled with animal validation revealed that the CHGX formula exhibited promising efficacy in alleviating systemic candidiasis through a multi-component, multi-target, and multi-pathway mechanism.

In this study, we identified 103 active components and 279 potential target genes associated with the CHGX formula (Figure 1). Additionally, we discovered 53 overlapping targets between the CHGX formula and systemic candidiasis (Figure 2A). Notably, key components of the CHGX formula, including quercetin, oleic acid, β-sitosterol, emodin and licochalcone A demonstrated robust binding affinities to core targets such as IL-6, TNF, and CXCL8 (Figure 5). Quercetin, a flavonoid abundant in *Glycyrrhiza uralensis* and *Pogostemon cablin*, has been shown to inhibit the production of pro-inflammatory cytokines such as IL-6, TNF-α and IL-8 by suppressing the NF-κB and MAPK signaling pathways.[18,19] Additionally, quercetin could enhance macrophage phagocytosis and promote Treg cell differentiation which is critical for inhibiting excessive inflammation and maintaining antifungal immunity.[20,21] Oleic acid has been

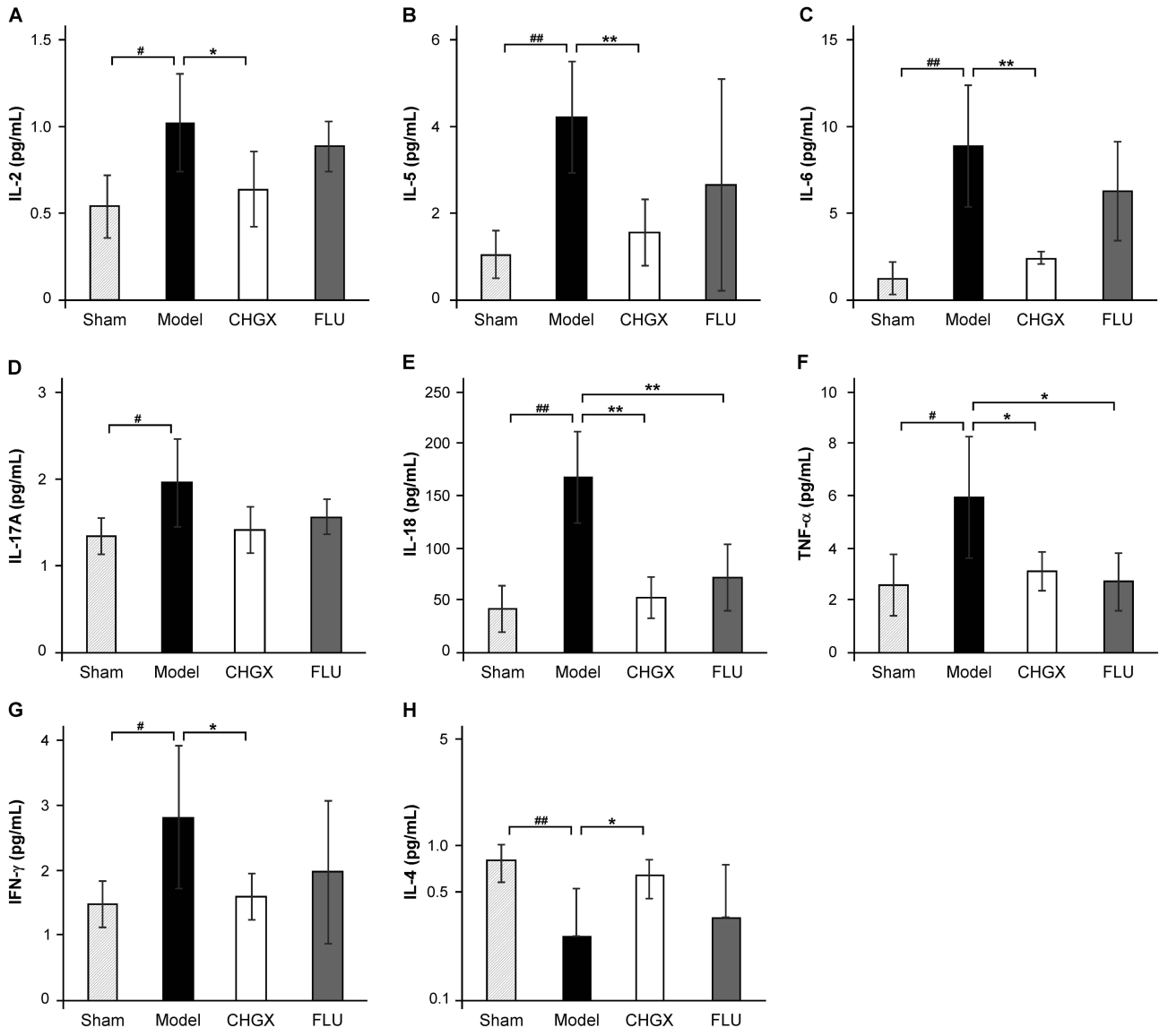

Figure 10 Effect of CHGX on cytokine expression in the serum of systemic candidiasis mice. (**A**–**G**) Inhibitory effects of CHGX on pro-inflammatory cytokines: IL-2, IL-5, IL-6, IL-17A, IL-18, TNF-α, and IFN-γ. (**H**) Promoting effect of CHGX on the anti-inflammatory cytokine IL-4. The data are presented as (mean ± SD). $^{\#}p < 0.05$ or $^{\#\#}p < 0.01$ indicate significant differences compared with the sham group. $^{*}p < 0.05$ or $^{**}p < 0.01$ indicate significant differences compared with the model group.

recognized for its ability to inhibit NLRP3 inflammasome activation. This inhibition occurs by reducing the secretion of IL-1β and IL-18, which are key mediators of pyroptosis in candidiasis.[21,22] Furthermore, our histopathological results indicate that CHGX formula could effectively reduce the level of inflammation in renal tissue, which may be closely related to the anti-inflammatory effect of its active ingredient oleic acid.

β-Sitosterol, a phytosterol from *Glycyrrhiza uralensis*, has been shown to inhibit TLR4/NF-κB signaling, reducing the release of IL-6 and TNF-α in sepsis models.[23] Our molecular docking analysis demonstrated a robust binding interaction between β-sitosterol and CXCL8, a chemokine that plays pivotal role in neutrophil recruitment.[24] By modulating and attenuating the biological activity of CXCL8 activity, β-sitosterol has the potential to mitigate neutrophil-mediated tissue damage during candidiasis. This finding aligns with our observed reduction in renal inflammatory infiltration, providing further support for the anti-inflammatory effects of CHGX formula. Emodin, a bioactive anthraquinone isolated from *Rheum palmatum*, has been demonstrated to erert antifungal effects by disrupting the integrity of the *Candida* cell membrane through binding to β-(1,3)-glucan synthase.[25,26] Additionally, it exhibits anti-inflammatory properties by suppressing Th17 cell differentiation via the inhibition of STAT3 signaling pathways.[27,28] Similarly, licochalcone A,

a flavonoid derived from *Glycyrrhiza uralensis*, is well-known for its dual antifungal and anti-inflammatory activities.[29–31] Studies have reported that licochalcone A inhibits hyphal formation and biofilm development in *C. albicans* by disrupting ergosterol biosynthesis.[30,31] Specifically, licochalcone A could downregulate the expression of RORγt, a transcription factor closely associated with Th17 cells, while upregulating the expression of Foxp3, a marker for regulatory T cells.[32] This mechanism provides a plausible explanation for the observed immunological alterations in mice treated with CHGX formula.

Enrichment analysis revealed that the CHGX formula is primarily involved in cytokine-mediated signaling pathways and biological processes associated with inflammatory regulation and immune cell activation (Figure 3). IL-17/Th17-mediated immunity plays a crucial role in defense against *C. albicans* infections, particularly mucocutaneous infections such as dermal and oral candidiasis.[33,34] IL-17A contributes to maintaining the integrity of the epithelial barrier and facilitating the recruitment of neutrophils to infection sites. Conversely, dysregulation of IL-17A has been shown to exacerbate inflammatory pathology in a murine model of candidiasis.[33] In addition, Tregs play a critial role in maintaining immune homeostasis by suppressing excessive inflammation and preventing immune-mediated tissue damage.[35,36] During *Candida albicans* infection, Tregs are essential for limiting excessive inflammation and tissue damage induced by Th17 and other pro-inflammatory responses.[37–39] In this study, CHGX treatment resulted in an reduction of Th17 cell populations and IL-17A levels, while significantly expanding Treg cell populations. These results suggest that CHGX formula may facilitate the restoration of immune homeostasis after infection, probably through the modulation of the Th17/Treg balance.

The Toll-like receptor (TLR) signaling pathway, particularly TLR2 and TLR4, plays an indispensable role in recognizing pathogen-associated molecular patterns (PAMPs) of *Candida* species.[40,41] Activation of TLR triggers the nuclear factor-κB (NF-κB) mediated production of pro-inflammatory cytokines, such as IL-6 and IL-1β, and primes adaptive immune responses.[42,43] Molecular docking results indicate that components of CHGX formula, including quercetin and emodin, may modulate TLR signaling by inhibiting the NF-κB pathway. This inhibition is likely to lead to a reduction in IL-6 and IL-1β levels, thereby attenuating early hyperinflammation in *Candida* sepsis.

Experimental validation confirmed the therapeutic potential of the CHGX formula. In murine models of systemic candidiasis, CHGX treatment significantly enhanced survival rates and reduced renal fungal burden (Figures 6 and 7). This beneficial effect was associated with alleviated kidney pathology, characterized by decreased edema, inflammatory infiltration, and fungal colonization. Mechanistically, CHGX formula promoted the recruitment of macrophage and expansion of Treg cell population, while simultaneously suppressing Th17-mediated inflammation responses (Figure 9). These findings demonstrate that CHGX formula exerts dual functions in enhancing antifungal immunity and mitigating immunopathology damage. Furthermore, the anti-inflammatory properties of CHGX were supported by decreased levels of key cytokines implicated in candidiasis-related organ injury, including IL-6, TNF-α and IFN-γ (Figure 10). Notably, CHGX treatment restored the levels of the cytokine IL-4, a crucial cytokine for alternative macrophage activation and tissue repair, highlighting its capacity to rebalance immune responses after infection.

Conclusion

In conclusion, our study provides valuable insights into the clinical application of TCM for fungal infection. The CHGX formula represents a multi-target therapeutic strategy against systemic candidiasis, exerting roles in immune regulation, anti-inflammatory and fungal clearance with its multi-components characteristics. These findings highlight the dual role of CHGX formula in both antifungal activity and host immune regulation, especially in the management of fungal infection in immunocompromised patients. However, several limitations require further investigation. Although CHGX improved survival rates and reduced the fungal burden in our model, its efficacy was inferior to that of fluconazole, indicating its potential role as an adjunctive therapy rather than a standalone treatment. In addition, our current study lacks molecular experimental validation, such as cellular thermal shift assay (CETSA) and western blot analysis, which are essential for confirming the molecular docking results and elucidating the regulatory roles of relevant signaling pathways. Thus, the underlying regulatory mechanisms of the identified targets and pathways need further validation.

Funding

This work was supported by the National Natural Science Foundation of China (Grant No. 82304963), the National Administration of Traditional Chinese Medicine Program of China (Grant No. zyyzdxk-2023001), and the Sanming Project of Medicine in Shenzhen (Grant No. SZZYSM202411012).

Disclosure

The authors report no conflicts of interest in this work.

References

1. Wisplinghoff H, Bischoff T, Tallent SM, et al. Nosocomial bloodstream infections in US hospitals: analysis of 24,179 cases from a prospective nationwide surveillance study. *Clin Infect Dis*. 2004;39(3):309–317. doi:10.1086/421946
2. Kullberg B, Arendrup M. Invasive candidiasis. *N Engl J Med*. 2015;373(15):1445–1456. doi:10.1056/NEJMra1315399
3. Data and Statistics on Candidemia. Available from: https://www.cdc.gov/candidiasis/data-research/facts-stats/index.html..
4. Magill SS, Edwards JR, Bamberg W, et al. Multistate point-prevalence survey of health care-associated infections. *N Engl J Med*. 2014;370 (13):1198–1208. doi:10.1056/NEJMoa1306801
5. Cowen LE, Sanglard D, Howard SJ, et al. Mechanisms of antifungal drug resistance. *Cold Spring Harb Perspect Med*. 2014;5(7):a019752. doi:10.1101/cshperspect.a019752
6. Sandai D, Tabana YM, Ouweini AE, et al. Resistance of Candida albicans biofilms to drugs and the host immune system. *Jundishapur J Microbiol*. 2016;9(11):e37385. doi:10.5812/jjm.37385
7. Lee Y, Puumala E, Robbins N, et al. Antifungal drug resistance: molecular mechanisms in Candida albicans and beyond. *Chem Rev*. 2021;121 (6):3390–3411. doi:10.1021/acs.chemrev.0c00199
8. Zhao G, Chen R, Li B, et al. Clinical practice guideline on traditional Chinese medicine therapy alone or combined with antibiotics for sepsis. *Ann Transl Med*. 2019;7(6):122. doi:10.21037/atm.2018.12.23
9. Yue H, Xu X, He S, et al. Antifungal mechanisms of a chinese herbal medicine, cao huang gui xiang, against Candida species. *Front. Pharmacol*. 2022;13:813813.
10. Yue H, Xu X, Peng B, et al. Antifungal activity of the dichloromethane extract of CaoHuangGuiXiang formula against Candida auris by in vitro and in vivo evaluation. *Infect Drug Resist*. 2024;17:3547–3559. doi:10.2147/IDR.S467418
11. Suvas PK, Setia M, Rana M, et al. Novel characterization of CXCR4 expressing cells in uninfected and herpes simplex virus-1 infected corneas. *Ocul Surf*. 2023;28:99–107. doi:10.1016/j.jtos.2023.02.006
12. He S, Zhao J, Xu X, et al. Uncovering the molecular mechanism of the qiang-Xin 1 formula on sepsis-induced cardiac dysfunction based on systems pharmacology. *Oxid Med Cell Longev*. 2020;2020:3815185. doi:10.1155/2020/3815185
13. Krysan DJ, Sutterwala FS, Wellington M. Catching fire: Candida albicans, macrophages, and pyroptosis. *PLoS Pathog*. 2014;10(6):e1004139. doi:10.1371/journal.ppat.1004139
14. Wellington M, Koselny K, Sutterwala FS, et al. Candida albicans triggers NLRP3-mediated pyroptosis in macrophages. *Eukaryot Cell*. 2014;13 (2):329–340. doi:10.1128/EC.00336-13
15. Richardson JP, Moyes DL. Adaptive immune responses to Candida albicans infection. *Virulence*. 2015;6(4):327–337. doi:10.1080/ 21505594.2015.1004977
16. Soriano A, Honore PM, Puerta-Alcalde P, et al. Invasive Candidiasis: current clinical challenges and unmet needs in adult populations. *J Antimicrob Chemother*. 2023;78(7):1569–1585. doi:10.1093/jac/dkad139
17. Naglik JR, Gaffen SL, Hube B. Candidalysin: discovery and function in Candida albicans infections. *Curr Opin Microbiol*. 2019;52:100–109. doi:10.1016/j.mib.2019.06.002
18. Oboh G, Ademosun AO, Ogunsuyi OB. Quercetin and its role in chronic diseases. *Adv Exp Med Biol*. 2016;929:377–387.
19. Tan RZ, Wang C, Deng C, et al. Quercetin protects against cisplatin-induced acute kidney injury by inhibiting Mincle/Syk/NF-κB signaling maintained macrophage inflammation. *Phytother Res*. 2020;34(1):139–152. doi:10.1002/ptr.6507
20. Wang Y, Wan R, Peng W, et al. Quercetin alleviates ferroptosis accompanied by reducing M1 macrophage polarization during neutrophilic airway inflammation. *Eur J Pharmacol*. 2023;938:175407. doi:10.1016/j.ejphar.2022.175407
21. Ke X, Chen Z, Wang X, et al. Quercetin improves the imbalance of Th1/Th2 cells and Treg/Th17 cells to attenuate allergic rhinitis. *Autoimmunity*. 2023;56(1):2189133. doi:10.1080/08916934.2023.2189133
22. Liu R, Tu M, Xue J, et al. Oleic acid induces lipogenesis and NLRP3 inflammasome activation in organotypic mouse meibomian gland and human meibomian gland epithelial cells. *Exp Eye Res*. 2024;241:109851. doi:10.1016/j.exer.2024.109851
23. Kasirzadeh S, Ghahremani MH, Setayesh N, et al. β-sitosterol alters the inflammatory response in CLP rat model of sepsis by modulation of NF-κB signaling. *Biomed Res Int*. 2021;2021:5535562. doi:10.1155/2021/5535562
24. Cambier S, Gouwy M, Proost P. The chemokines CXCL8 and CXCL12: molecular and functional properties, role in disease and efforts towards pharmacological intervention. *Cell Mol Immunol*. 2023;20(3):217–251. doi:10.1038/s41423-023-00974-6
25. Janeczko M, Masłyk M, Kubiński K, et al. Emodin, a natural inhibitor of protein kinase CK2, suppresses growth, hyphal development, and biofilm formation of Candida albicans. *Yeast*. 2017;34(6):253–265. doi:10.1002/yea.3230
26. Janeczko M. Emodin reduces the activity of (1,3)-β-D-glucan synthase from candida albicans and does not interact with caspofungin. *Pol J Microbiol*. 2018;67(4):463–470. doi:10.21307/pjm-2018-054
27. Zhou Q, Xiang H, Liu H, et al. Emodin alleviates intestinal barrier dysfunction by inhibiting apoptosis and regulating the immune response in severe acute pancreatitis. *Pancreas*. 2021;50(8):1202–1211. doi:10.1097/MPA.0000000000001894
28. Semwal RB, Semwal DK, Combrinck S, et al. Emodin - A natural anthraquinone derivative with diverse pharmacological activities. *Phytochemistry*. 2021;190:112854. doi:10.1016/j.phytochem.2021.112854

29. Hao H, Hui W, Liu P, et al. Effect of licochalcone A on growth and properties of Streptococcus suis. *PLoS One*. 2013;8:e67728. doi:10.1371/journal.pone.0067728
30. Shahzad M, Sherry L, Rajendran R, et al. Utilising polyphenols for the clinical management of Candida albicans biofilms. *Int J Antimicrob Agents*. 2014;44(3):269–273. doi:10.1016/j.ijantimicag.2014.05.017
31. Seleem D, Benso B, Noguti J, et al. In vitro and in vivo antifungal activity of lichochalcone-A against Candida albicans biofilms. *PLoS One*. 2016;11(6):e0157188. doi:10.1371/journal.pone.0157188
32. Liu M, Du Y, Gao D. Licochalcone A: a review of its pharmacology activities and molecular mechanisms. *Front Pharmacol*. 2024;15:1453426. doi:10.3389/fphar.2024.1453426
33. Conti HR, Shen F, Nayyar N, et al. Th17 cells and IL-17 receptor signaling are essential for mucosal host defense against oral candidiasis. *J Exp Med*. 2009;206(2):299–311. doi:10.1084/jem.20081463
34. Conti HR, Gaffen SL. Host responses to Candida albicans: th17 cells and mucosal candidiasis. *Microbes Infect*. 2010;12(7):518–527. doi:10.1016/j.micinf.2010.03.013
35. van de Veerdonk FL, Kullberg BJ, Netea MG. Pathogenesis of invasive candidiasis. *Curr Opin Crit Care*. 2010;16(5):453–459. doi:10.1097/MCC.0b013e32833e046e
36. Whibley N, Gaffen SL. Brothers in arms: th17 and Treg responses in Candida albicans immunity. *PLoS Pathog*. 2014;10(12):e1004456. doi:10.1371/journal.ppat.1004456
37. De Luca A, Montagnoli C, Zelante T, et al. Functional yet balanced reactivity to Candida albicans requires TRIF, MyD88, and IDO-dependent inhibition of Rorc. *J Immunol*. 2007;179:5999–6008. doi:10.4049/jimmunol.179.9.5999
38. Bonifazi P, Zelante T, D'Angelo C, et al. Balancing inflammation and tolerance in vivo through dendritic cells by the commensal Candida albicans. *Mucosal Immunol*. 2009;2:362–374. doi:10.1038/mi.2009.17
39. Whibley N, Maccallum DM, Vickers MA, et al. Expansion of Foxp3(+) T-cell populations by Candida albicans enhances both Th17-cell responses and fungal dissemination after intravenous challenge. *Eur J Immunol*. 2014;44:1069–1083. doi:10.1002/eji.201343604
40. Salgado RC, Fonseca DLM, Marques AHC, et al. The network interplay of interferon and Toll-like receptor signaling pathways in the anti-Candida immune response. *Sci Rep*. 2021;11(1):20281. doi:10.1038/s41598-021-99838-0
41. Viens AL, Timmer KD, Alexander NJ, et al. TLR signaling rescues fungicidal activity in Syk-deficient neutrophils. *J Immunol*. 2022;208(7):1664–1674. doi:10.4049/jimmunol.2100599
42. Netea MG, Joosten LAB, van der Meer JWM, et al. Immune defense against Candida fungal infections. *Nat Rev Immunol*. 2015;15:630–642. doi:10.1038/nri3897
43. Liu J, Geng F, Sun H, et al. Candida albicans induces TLR2/MyD88/NF-κB signaling and inflammation in oral lichen planus-derived keratinocytes. *J Infect Dev Ctries*. 2018;12(9):780–786. doi:10.3855/jidc.8062